Journal of Materials Chemistry A

ROYAL SOCIETY OF CHEMISTRY

PAPER

View Article Online
View Journal | View Issue

Cite this: J. Mater. Chem. A, 2025, 13, 37528

Hydrophobic silsesquioxane-modified lignin-incorporated polyurethane film

Banchamlak Bemerw Kassaun,[a] Yu Liu,[b] Fangong Kong*[b] and Pedram Fatehi *[ac]

Received 19th June 2025
Accepted 1st October 2025

DOI: 10.1039/d5ta04986e

rsc.li/materials-a

Polyurethane (PU) is widely used in adhesive, foam, and coating applications. Currently, there is an urgent need to enhance PU's hydrophobic, thermal, and flame-retardant properties to improve its performance while minimizing its environmental impact. In this work, we introduce a new recyclable PU-derived composite film with enhanced superhydrophobicity and flame retardancy. The coating formulation consisted of 50 wt% water-based silsesquioxane lignin (WL) as a superhydrophobic constituent, 0.12 wt% sulfoethylated lignin (SL) as a dispersant, and 1 wt% epoxidized oil as a plasticizer. The aqueous-based PU film exhibited superhydrophobic performance (164° ± 2° water contact angle and 4° ± 2° low sliding angle) and enhanced mechanical strength. Flame-retardant analysis indicated a limiting oxygen index improvement from 18.5% in pure PU to 25.5% in the lignin-incorporated PU formulation. The formulation demonstrated superhydrophobic and flame-retardant improvement when coated over wood, metal, and paper surfaces, and these properties were resistant to sandpaper abrasion, UV ozone exposure, and thermal exposure. This aqueous phase polyurethane (PU) formulation is suitable for coating various surfaces with environmentally benign properties.

1. Introduction

Polyurethane (PU) is a polymer made of isocyanate (a hard segment) and polyol (a soft segment) to form a repeating urethane group.[1] Due to its high substrate adhesion and mechanical properties, PU is utilized in various applications, including adhesives, coatings, adsorbents, and elastomers.[2] Nevertheless, PU exhibits poor waterproofing and thermal stability.[3] In PU formulation, polar groups and hydrophilic components affect water repellency, resulting in poor hydrophobicity.[4] In addition, PU's urethane linkages are susceptible to oxidation and hydrolysis, rendering it thermally unstable.[5,6] Due to its significant flammability and limited hydrophobic properties, the application of PU on wood coatings is limited.[5] Moreover, the use of non-renewable, petroleum-based ingredients in PU fabrication is known to be environmentally unfriendly.[6] The hydrophobic properties of PU materials were reported to be improved by decreasing surface energy and generating rough surfaces utilizing silicide and fluoride.[7,8] Despite its acceptable flame retardancy, fluoride in PU may have adverse environmental implications and, thus, is not suitable for the PU application.[9] Currently, the PU industry seeks ways to reduce its environmental impact while improving PU products' hydrophobicity and thermal properties.[6,10]

Lignin is a natural polymer and can be utilized in PU composites to enhance their properties and reduce their environmental impact.[11] Lignin is highly favorable for PU composites due to its abundance and multi-functionality.[11] Adding lignin to PU composites improves PU's resistance to heat and flammability by promoting the formation of char layers.[12,13] In addition, due to the strong hydrogen bonding between lignin's hydroxyl groups and the PU's urethane groups, lignin may improve the tensile strength, modulus, and elongation at the break of the matrix at a low dosage (<5 wt%).[14,15] However, lignin-based PU composites still face challenges at a higher dosage, which stem primarily from inadequate dispersion of lignin in the PU matrix. Such a heterogeneous dispersion would compromise the composition uniformity of the PU matrix and subsequently diminish the hydrophobicity and mechanical integrity of the matrix.[16] Some common strategies to improve the interfacial adhesion and dispersion of lignin in the PU matrix are lignin nanoparticle production,[17,18] chemical modification of lignin,[19–21] and the addition of compatibilizers in the PU-lignin matrix.[22] For example, wheat straw-based lignin nanoparticles were utilized as nanofillers in the PU film production,[17] and their 5 wt% inclusion improved the water contact angle of the PU film by 49° and increased tensile strength by 36%. However, the two-step modification of lignin may be economically unviable for the larger-scale implementation of this strategy. In another investigation, the addition of 0.5 wt% 3-aminopropyltriethoxy silane (APTES)-

[a]Green Processes Research Centre and Chemical Engineering Department, Lakehead University, 955 Oliver Road, Thunder Bay, ON P7B5E1, Canada. E-mail: pfatehi@lakehadu.ca

[b]State Key Laboratory of Biobased Material and Green Papermaking, Qilu University of Technology, Shandong Academy of Sciences, Jinan 250353, China. E-mail: kfg@qlu.cn

[c]Laboratory of Natural Materials Technology, Åbo Akademi University, Henrikinkatu 2, Turku, FI-20500, Finland

functionalized lignin to PU films resulted in a 9% increase in tensile strength and improved thermal stability.[21] Also, recent studies highlight the beneficial impact of lignin's antioxidant and UV-blocking properties in fabricating protective coating from PU-polydimethylsiloxane (PDMS) composites.[23,24] In this case, lignin can act as a reinforcing filler in PU-PDMS, improving hydrophobicity and UV resistance of the composite for applications like steel and plank coatings.[25] Alternatively, lignin serves as a sustainable crosslinker, reducing the need for petro-based crosslinkers, while maintaining the thermal stability of composites. For example, low molecular weight lignin was employed to synthesize a lignin-based waterborne polyurethane (LWPU) *via* incorporating polycaprolactone diol (PCL) and polydimethylsiloxane (PDMS) for use in paper coatings.[26] The resulting LWPU films demonstrated impressive mechanical performance, achieving a peak tensile strength of 40.3 MPa and an extraordinary elongation at break of 1148%.[26] In addition to being hydrophobic, the films showed resistance to aging and provided UV protection.[26] These findings highlight lignin's potential to improve the characteristics of PU-PDMS composite in diverse applications. However, challenges related to lignin's structural variability and limited compatibility with PU pose obstacles to its application in the PU matrix. As stated earlier, at a higher dosage of lignin, the strength and thermal properties of the PU composite film drop due to poor dispersion and aggregation of lignin in the formulation.[16] Hence, it is necessary to determine a pathway to incorporate lignin in the production of PU film at a higher concentration while improving the mechanical, thermal, and hydrophobic characteristics of PU films.

Enhancing the recyclability of PU materials offers an additional approach to mitigate their environmental impact.[25,26] The recyclability of PU materials is significantly influenced by their diisocyanate and polyol components. Furthermore, certain additives and fillers can enhance or hinder the recyclability of PUs by affecting their resistance to heat and degradation. Hence, the meticulous choice and enhancement of polyurethane components are essential for improving their potential recyclability and sustainability. The introduction of lignin in PU materials is reported to improve their re-processability.[27,28] In this work, we aim to produce PU materials that are highly functional (fire resistant and superhydrophobic) and recyclable.

We present a concise and environmentally conscious approach for synthesizing water-based polyurethane (PU) coating materials that incorporate softwood kraft lignin. This approach exploits two separate lignin modifications of a water-based silsesquioxane lignin copolymer (WL) obtained through the copolymerization of lignin with aminopropyl/methyl silsesquioxane (WAPMSS) and sulfoethylated lignin (SL), achieved *via* sulfoethylation of lignin with 2-bromoethanesulfonate. The WL was utilized as a superhydrophobic and flame-retardant ingredient, while the SL served as a dispersant in the PU formulation. In opposition to traditional PU/lignin composites, the composite manufacturing process was solvent- and catalyst-free. The resultant materials with high lignin incorporation (up to 50%) exhibited superior water repellency, high thermal stability, processability, improved flame retardancy, and recyclability. Further investigations revealed that the resultant material can be utilized in high-abrasive environments while maintaining its superhydrophobicity.

2. Result and discussion

2.1. Structural insight of lignin derivatives

Sulfoethylated lignin (SL) and lignin-silsesquioxane copolymer (WL) were produced from kraft lignin (KL) through the substitution of phenolic hydroxyl groups with 2-bromoethansulfonate and the replacement of the hydroxyl group with a siloxane bond using aminopropyl/methyl silsesquioxane, respectively, as displayed in Fig. S1a and b in the SI.[29] NMR, XPS, and FTIR studies were conducted on KL, SL, and WL to ascertain their respective chemical structures. Fig. S2–S5 illustrate the spectra of the biopolymers, along with the structural representation of a monomeric unit, and Table 1 illustrates the summary of the Figures' outcomes. As observed in the ^{1}H-NMR and HSQC NMR analyses, the lignin derivatives contained aromatic and methoxy protons, as well as β-O-4, β-5, and β-β linkages, with varying proportions.[30–33] This finding indicates that both WL and SL kept the original structure of KL.[34] A novel bond of –O–CH_2, CH_2–S–O, S═O, and SO_3H was observed in the SL polymer, which was attributed to the sulfoethylation modification (Table 1).[29] The presence of –OH–Si, NH_2, CH_2–CH_2–CH_2, and CH_3–Si groups in WL is attributed to the peaks originating from silsesquioxane copolymerization.[35] In addition, the presence of C–O–Si signals observed in NMR, FTIR, and XPS spectra of WL confirms a condensation reaction involving WAPMSS and KL.[36] The XPS analysis confirms the presence of silicon and nitrogen in WL, which didn't exist in KL or SL in Fig. S4a.[37–39]

The proportions of aliphatic, aromatic, and carboxylate hydroxyl (OH) groups present in the samples are quantified and depicted in Table 1. The hydroxyl group content of the SL polymers was lower than that of KL, whereas no hydroxyl groups were discernible for WL (Fig. S2c). The decrease in the overall number of hydroxyl groups in SL provides evidence for the successful transformation of the hydroxyl groups of KL, which is further corroborated by the presence of C–O–C connections in HSQC NMR analysis. Similarly, the silanization process resulted in the complete conversion of the hydroxyl groups of KL for WL production (Fig. S2). This analysis confirms the success of KL conversion to SL and WL, as shown in Fig. 1.

2.2. Effect of lignin-silsesquioxane copolymer on the stability of PU emulsion

The assessment of the coating formulation's stability provides insights into the interactions of its constituents and the shelf life of the formulation.[40] The formulation was prepared by combining a PU water emulsion with varying proportions of WL or KL. The appearance of dispersion stability (*i.e.*, TSI global index) of the five samples over 12 hours is shown in Fig. S6 and S7a. An inverse relationship exists between the stability of a coating formulation and the TSI value, whereby an increase in stability corresponds to a decrease in the TSI value.[41] The PU

Table 1 Structural components of KL, SL, and WL as identified by NMR, XPS, and FTIR

Polymer	Functional groups/ protons, ^{1}H NMR (ppm), (ref. 43)	HSQC cross-peak signals, δ_C/δ_H (ppm) (ref. 44)	^{31}P NMR hydroxyl groups (ppm), mmol g^{-1} (ref. 45)	XPS, (eV) (ref. 46)	FTIR, (cm^{-1}) (ref. 47)
KL	DMSO-d_6 (2.5), aromatic (6.0–7.5), methoxy (3–4), aliphatic (0–3.2)	β-O-4 (71.4/4.7), β-5 (53.29/3.44) β-β (53.6/3.0) Methoxy (55.5/3.70)	Aliphatic (150–145), 2.15 aromatic (144–137.5), 3.92 Carboxylic-OH (136–132), 0.76	C 1s (285), O 1s (532), S 2p (166.5), C–C (284.8), C=O (288–290), C–O (286)	Aromatic and aliphatic-OH (3340)
SL	DMSO-d_6 (2.5), aromatic (6.0–7.5), methoxy (3–4), aliphatic (0–3.2), –O–CH_2 (3.2)	β-O-4 (71.4/4.7), β-5 (53.29/3.44), β-β (53.6/3.0), OCH_2 (0.7/2.8), CH_2 (32.2/1.8)	Aliphatic (150–145), 2.45, aromatic (144–137.5), 2.45, carboxylic (136–132), 0.67	C 1s (285), O 1s (532), S 2p (166.5), C–C (284.8), C=O (288–290), C–O (286), C–S (284.8), S=O (168), S–H (163), and S–O (165)	Aromatic and aliphatic-OH (3340), SO_3H (1080)
WL	5 (D_2O), 2.7 (–OH from silicon), 1.5 (NH_2), 0.5 (CH_2–CH_2–CH_2), 0 (CH_3–Si)	C–O–Si (46.2/3.2)	Not identified	C 1s (285), O 1s (532), S 2p (166.5), Si 2p (152.9), N 1s (400) C–C (284.8), C=O (288–290), C–O (286), C–Si (283), Si–C (101.34 eV), Si–O–Si/Si–OH (103.76), and Si–O–C (102.5)	Si–OH (3750), Si–CH_3 (835 and 785), Si–O–Si (1008 and 1000), Si–C–H (3005)

emulsion was stable, as evidenced by a TSI value of 2. Adding KL elevated the TSI value, suggesting a less stable system.

Similarly, the inclusion of WL polymer in the PU emulsion system resulted in a significant increase in the TSI value. KL has superior dispersion to WL in the PU matrix, as evidenced by the TSI results and corroborated through naked eye inspection (Fig. S6). This suggests that the WL particles exhibit a greater hydrophobic interaction, leading to their aggregation and sedimentation.

2.3. Performance of PU film containing lignin-silsesquioxane copolymer

The examination conducted by XPS focused on analyzing the elemental compositions and chemical bonding characteristics of the films, specifically those of PU, PKL10, and PWL10 in Fig. 2a. The deconvolution of the C 1s peaks corresponding to the PU and PKL10 results in the identification of four main components: C–C (284.8 eV), C–N (286.2 eV), C=O (288–290 eV), and C–O (286 eV).[42]

The percentage area concentration of the C=O bond on PU is 2.10, whereas PKL10 has a concentration of 3.82. A considerable number of C=O bonds may indicate the existence of carboxylic-OH groups, which are notably abundant in the KL structure (Fig. S2c and S4b). An extra component, C–Si (283 eV), was observed in the deconvolution of PWL10. The presence of a C–Si bond in PWL10 indicates the existence of Si–CH_2 structural components originating from WL due to copolymerization (Fig. S4b). Fig. 2b and S7b display the stress–strain curves for the films, and datasets for tensile strength and elongation at break are illustrated in Fig. S7c and d.

The KL sample with a proportion of more than 10 wt% in PU displayed disintegration and fragility, making it impossible to analyze its mechanical properties, as depicted in Fig. S8. The insufficient film formation of KL at higher concentrations is attributed to aggregation resulting from significant self-

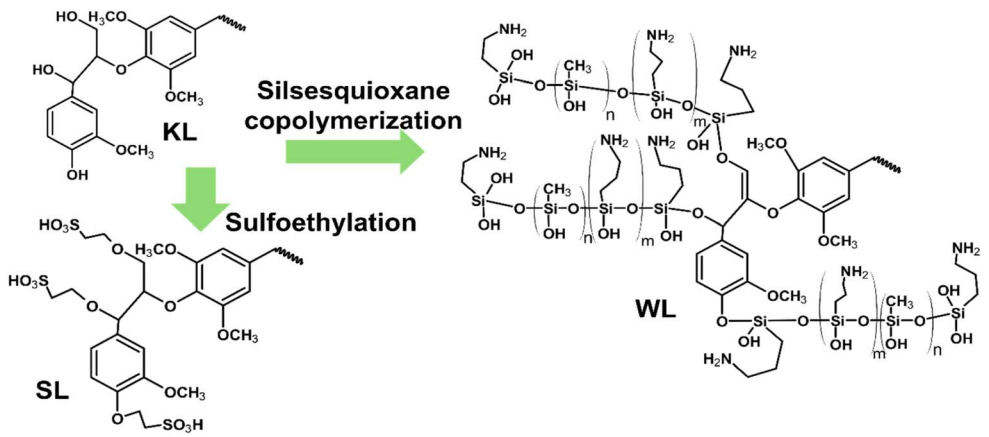

Fig. 1 The transformation of KL to SL and WL *via* sulfoethylation and silsesquioxane copolymerization.

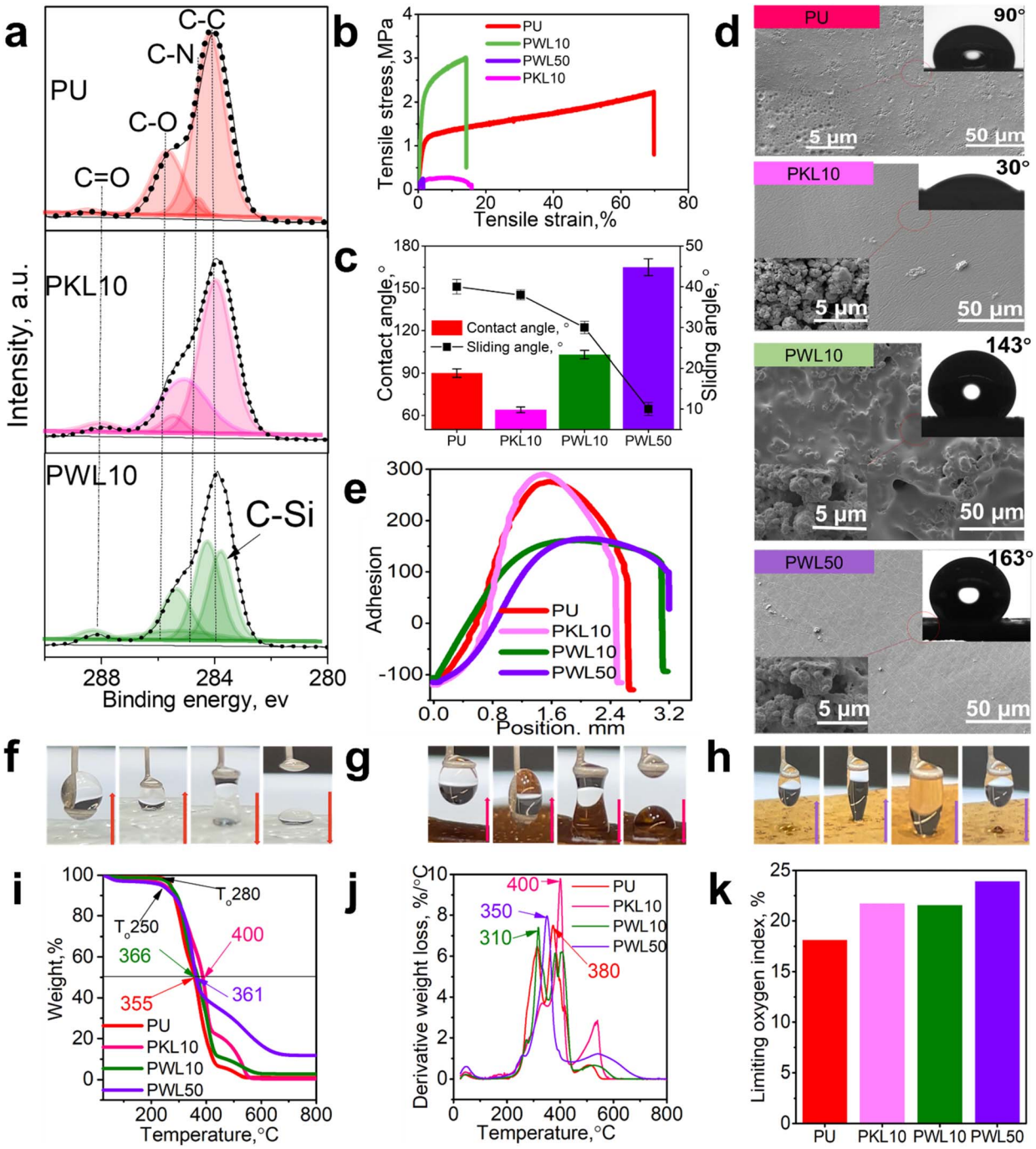

Fig. 2 C 1s deconvoluted XPS spectra of the films (a), stress–strain curves (b), water contact, and sliding angle (c) SEM images at 50 μm and 5 μm scales (d), water droplet adhesion force (e), droplet attachment and detachment steps on PU (f) and PKL10 (g) and PWL50 (h), and TGA (i), DTG (j) and limiting oxygen index (LOI) (k) of PU, PKL10, PWL10 and PWL50 films.

interaction.[48] Compared to PU, the WL and KL composite films exhibited reduced tensile strength and elongation at break.

However, incorporating lignin polymer resulted in an increased modulus, indicating that the produced film was more rigid.

Water contact angle (WCA) and sliding angle (SA) analysis were carried out to determine the superhydrophobic and hydrophobic characteristics of the films in Fig. 2c. The WCA and SA values of the pure PU were measured to be 90° and 40°, respectively. The 10 wt% KL inclusion in the PU matrix led to a reduction in WCA value by 35°.

Compared to the PU film, the hydrophilicity of the PKL10 film may be attributed to a free carboxylic group inside the PKL10 film structure (Fig. 2a). However, the water contact angle of PWL10 composites exhibited a 30° increase compared to pure PU. Furthermore, when the content of WL increased in the PU

film, the water contact angle increased while the SA decreased progressively. The PWL50 film exhibited the maximum WCA value of 163° and a low SA of 8°. The enhanced hydrophobicity of WL-containing films in comparison to PU may be attributed to the inclusion of a C–Si component in the PWL10 and PWL50 films (Fig. 2a), as well as the decreased concentration of C=O (0.6% area).[49]

To enhance comprehension and establish a connection between the surface morphology of the films, SEM imaging analysis of the samples was conducted (Fig. 2d). PU film surfaces were relatively smoother than those of PKL10 or PWL10. When KL particles were introduced to the PU matrix, the film surface exhibited microscopic clusters and clumps of particles. However, a more detailed examination reveals that these clusters were spherical aggregates. Conversely, the PWL10 film exhibited higher polymer aggregation than the PKL10 film, thus the lower mechanical properties (Fig. 2b).[50] The decreased dispersibility of the WL within the PU matrix is the cause of this discrepancy (Fig. S7a). The PWL10 and PWL50 films contained spherical macroscopic particles, as well as smaller particles and air pockets. This can be ascribed to the film's heightened hydrophobic nature and coating. Incorporating 50 wt% of WL into the PU matrix resulted in a smoother surface than incorporating 10 wt% (Fig. 2d).

Particle aggregates arranged diagonally on the PWL50 film were detected at reduced resolution, potentially contributing to the film's decreased mechanical characteristics (Fig. 2b). The poor dispersion of WL in the PU matrix suggests inadequate interfacial adhesion between the polymer matrix (PU) and WL, leading to reduced mechanical load transfer from the polymer matrix to WL and consequently resulting in poor mechanical characteristics of the overall film.[51]

Tensiometer assessments of water adhesion force were used to quantify the coatings' water adhesion force, as shown in Fig. 2e. The droplet profile was captured by a digital camera and presented in Fig. 2f–h. The instrument stage supported the suspended droplet when it contacted the sample on the stage, resulting in a considerably reduced force. As the stage dropped, the force rapidly increased until it reached its peak. The PU and PKL10 films exhibited detachment peaks at 1.5 and 2 mm, with pull-off forces of 250 μN and 285 μN, respectively. Like PWL50, the superhydrophobic film exhibited a detachment peak of 0.12 mm and a pull-off force of 80 μN. Hydrophobic surfaces, once separated, exhibit a notable decrease in adhesion force,[50] indicating that half of the droplet remains on the surface, as observed with PU and PKL10.

Conversely, PWL50 restored its water adhesion force to zero, demonstrating the extraordinary water-repellent and low water adhesion properties of such surfaces. The water droplet exhibited a strong adhesion to the surface of the PU (f) and PKL10 (g) films. However, the droplets could quickly detach from the PWL50 film (h) in Fig. 2. Films incorporated with WL exhibited high water repellency and resistance to water adhesion. This phenomenon may occur due to the copolymerization process, which would replace the hydrophilic hydroxy groups of lignin with hydrophobic silsesquioxane groups (Fig. S2). The WCA and SA (Fig. 2c) and SEM (Fig. 2d) revealed the presence of a hierarchical structure at both the micro- and nano-levels, coupled with the surface chemistry (presence of Si–C) (Fig. 2a), which contributed to enhanced superhydrophobic characteristics.

The thermal stability of PU, PKL10, PWL10, and PWL50 was investigated by TGA analyses, as shown in Fig. 2i and j. The film's thermal stability was assessed by the onset temperature (T_o), 50% weight loss temperature ($T_{50\%}$), and maximum decomposition temperature (DTG_{max}). PU showed T_o at 280 °C and $T_{50\%}$ at 355 °C. PKL10 had $T_{50\%}$ and DTG_{max} that were 45 °C and 20 °C higher than those of PU, respectively. Incorporating KL in the PU matrix significantly enhanced the thermal stability of the film. Adding more hard segments (aromatic structures of lignin) could result in the formation of crosslinks, leading to higher char production and enhanced interaction between the PU matrix and KL polymer.[52,53] The $T_{50\%}$ value of PWL10 decreased by 10 °C, whereas the DTG_{max} occurred 40 °C lower than PU. Poor WL dispersion (Fig. S7a) led to aggregation in the PU matrix (Fig. 2d). Agglomerations or clusters could cause film flaws or voids, and faults or voids in the PWL10 and PWL50 layers might lead to thermal deterioration.[54] The poor dispersion of WL (Fig. S7a) may reduce the contact area and interaction between the WL and the PU matrix, thereby compromising the WL's thermal barrier characteristics. Similarly, PWL50 film had a DTG_{max} of 350 °C, *i.e.*, 20 °C lower than PU film in Fig. 2j. Due to WL's inorganic component, PWL50's ultimate weight residue was 17% greater than PU's.

The limiting oxygen index (LOI) values of the films are illustrated in Fig. 2k. The pure PU had the lowest LOI value of 18.4%, while the PWL50 had the highest LOI value of 25.4%, exceeding the values of the other samples.

The WL-containing PU films exhibited a higher LOI than PU and PKL10, which was attributed to the enhanced charring properties of WL, as indicated by TGA analysis in Table S1. A silsesquioxane structure on the KL backbone provided thermal protection *via* enhanced charring and lowered flammability at high temperatures. When incorporated into a polyurethane (PU) polymer, silsesquioxane delays ignition and strengthens the PU matrix.[55] The WL polymer in water-based PU emulsion exhibited superior hydrophobicity, thermal stability, and flame-retardant features when utilized in a high concentration (50%), surpassing the performance of pure PU or PKL10 coating materials. Nevertheless, the mechanical characteristics of this film were significantly inferior to those of PU or PKL10 due to the inadequate dispersibility of WL in the PU matrix. Hence, an attempt was made to enhance the dispersibility of WL in the PU matrix by utilizing SL as a dispersant, as described in the following section.

2.4. Effect of sulfoethylated lignin on the stability of PU emulsion containing lignin-silsesquioxane copolymer

The effect of SL on the stability and surface properties of PWL50 formulation was investigated, and the results are shown in Fig. 3a–d. Fig. 3a shows that the absence of SL in the PWL50 sample resulted in instability, with a TSI value of 55. The high molecular weight (Table S1) and hydrophobic character of WL

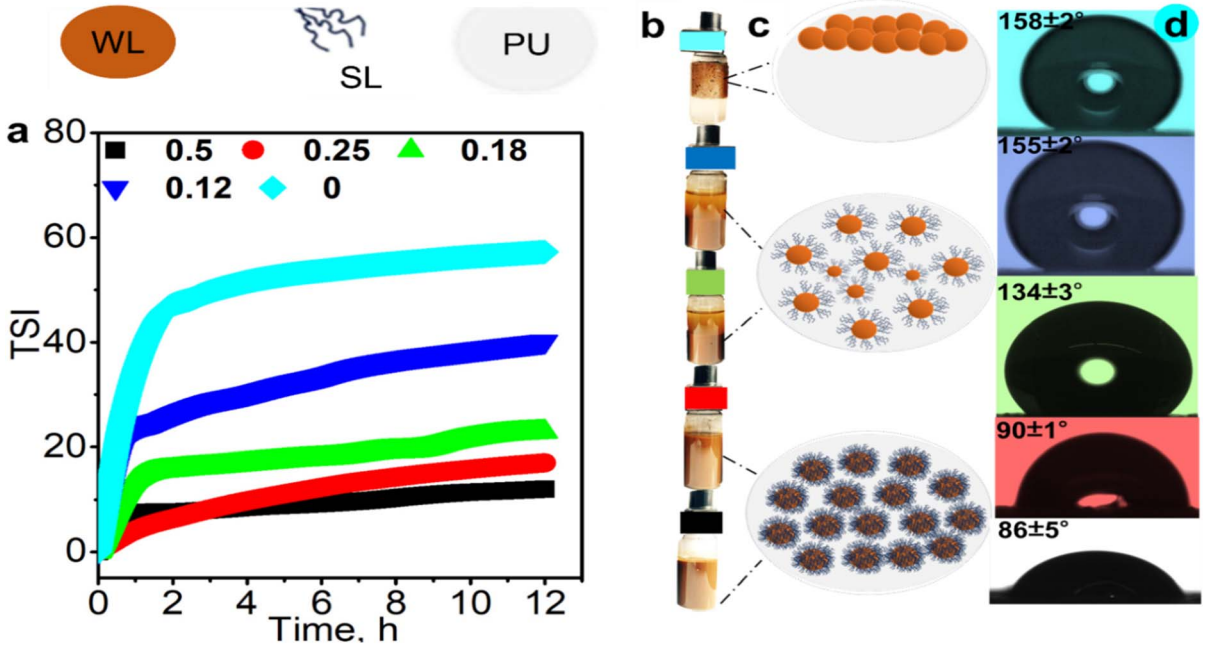

Fig. 3 Coating formulation stability (TSI) for 12 h every 30-second scan legend showing the concentration of SL (a), visual of the formulations after 12 h preparation (b), possible illustration of hydrophobic/hydrophilic effect of SL molecules in PWL50 dispersion (c) and water contact value of the films (d).

particles may hinder their dispersion in PU due to aggregation. Adding 0.12 wt% of SL to PWL50 increased dispersion stability by 25%, and adding more SL to the dispersion further improved its stability. However, the surface became more hydrophilic. These effects have also been found in previous investigations involving the utilization of sulfonated lignin as a dye dispersant.[56] Dispersants reduced particle agglomeration by introducing steric hindrance and electrostatic forces. Due to its high surface charge density (2.1 mmol g^{-1}), SL adsorption onto WL particles could prevent WL agglomeration by electrostatic repulsion (Fig. 3c). Introducing SL at lower concentrations (*e.g.*, 0.12 wt%) resulted in sustained superhydrophobicity with a contact angle of 155° (Fig. 3d). As a result, the 0.12 wt% concentration of SL was selected as a dispersant for the following section.

2.5. Effect of sulfoethylated lignin on lignin-silsesquioxane copolymer containing PU film characteristics

The effect of SL dispersant on the surface morphology, mechanical properties, and thermal properties of WL and KL-containing films was investigated, and the results are presented in Fig. 4. Fig. 4a illustrates the appearance and the surface morphology of films generated with the addition of 0.12 wt% SL. The addition of SL to a pure PU (PS) water emulsion changed the color from clear to brown, and the appearance of small aggregates was observed in the film; the WCA remained at 90°. Similarly, SL was incorporated in the KL and WL-containing formulas, where its addition improved the film's appearance while not affecting the water contact angle values, crediting the optimization of SL (Fig. 3a). The overall water absorption of the films was also analyzed using a tensiometer, as shown in Fig. 4b. PKL10S and PS exhibited the most water absorption, with 12.8 g g^{-1} and 11.8 g g^{-1}, respectively. PU had a lower water absorption compared to PKL10S and PS.

On the other hand, PWL10S and PWL50S exhibited the lowest water absorption, with values of 1 g g^{-1} and 2.1 g g^{-1}, respectively.

The reduced water absorption of PWL10S and PWL50S can be attributed to the films' higher water contact angle (WCA) values (Fig. 2d and 4a) and their hydrophobic characteristics. The greater water absorption of PWL50S, as opposed to PW10S, can be attributed to the exposure of the PU matrix in PWL50S, which is caused by the porous nature of the film. Fig. 4c shows the UV-transmittance spectra of the films; the PU films show more than 68% in the UVC (200–275 nm) regions, 78% transmittance in the UVB (275–320 nm) regions, and 90% transmittance in the UVA (320–380 nm) regions.

The films containing lignin exhibit 100% protection against UVA, UVB, and UVC radiation, as indicated by 0% transmittance in these regions. The superior UV-shielding property resulted from the abundant phenolic hydroxyl, methoxy, and carbonyl groups concentrated in the outer surface of KL, SL, and WL particles (Fig. S2 and S3). Additionally, the complex structure of lignin allowed for the scattering and absorption of UV light that penetrates the film, resulting in reduced transmittance.[57]

The stress–strain curve, tensile strength, and percentage elongation of PS, PKL10S, PWL10S, and PWL50S composite films are presented in Fig. 4d and S7c–e, respectively. Compared with films prepared without SL, the films generated with SL had a higher modulus and tensile strength. Incorporating SL in the pure PU film improved the tensile strength by 2.5 MPa. The

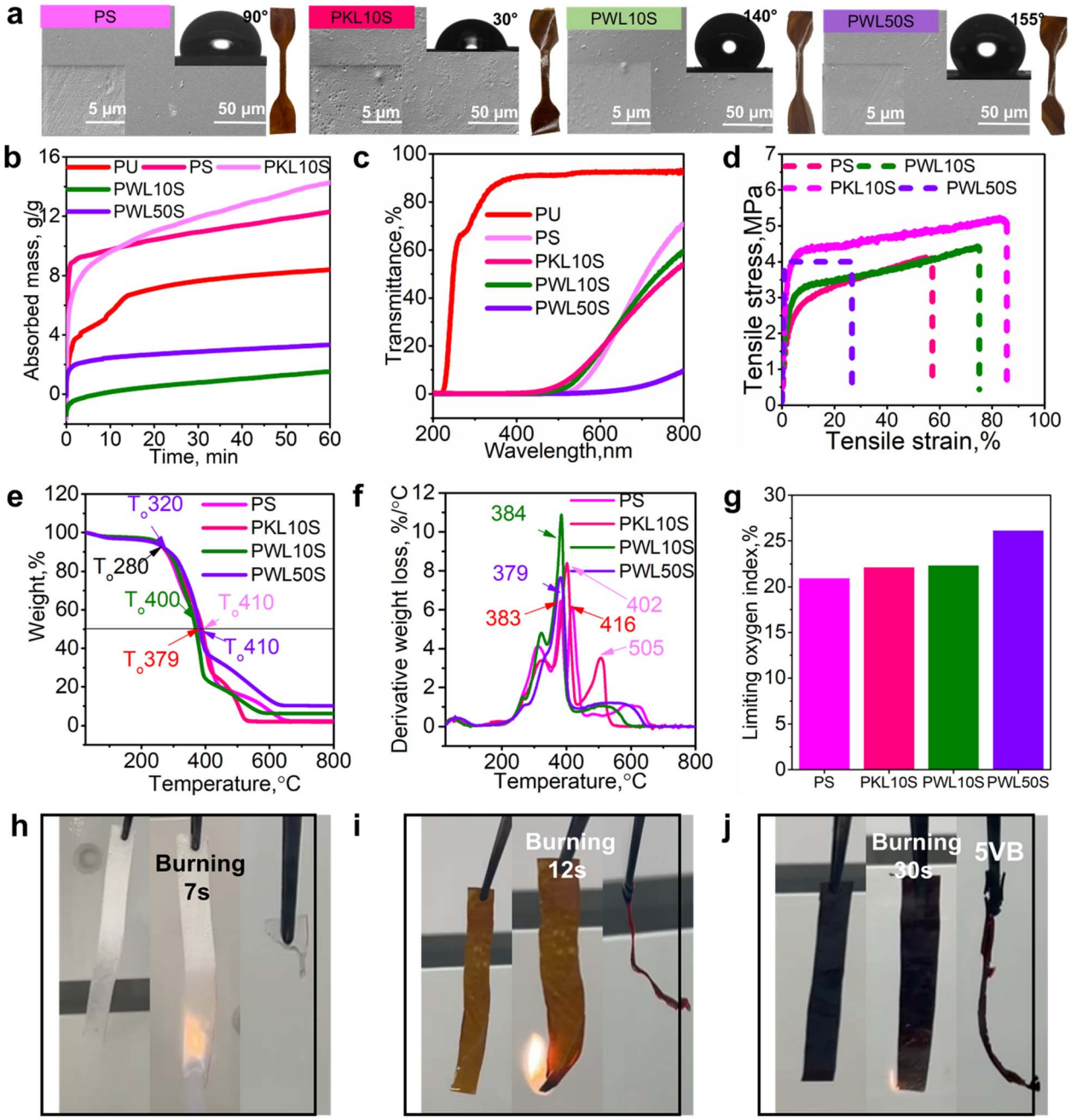

Fig. 4 Surface morphology, contact angle and appearance of films (a), water absorption (b), UV-vis transmittance spectra (c) stress–strain curve (d), TGA (e), DTG (f), limiting oxygen index (LOI) (g) of PS, PKL10S, PWL10S and PWL50S, digital images for the UL (98) test PU (h), PS (i), and PWL50S (j) of the films.

structural component of SL consisted of many aromatic structures (Fig. S2) that strengthen the films as rigid segments. PKL5S showed the highest tensile strength (32 MPa). Similarly, the PWL5S films exhibited an improvement in tensile strength of 9.5 MPa compared to PWL5.

This improvement in the tensile strength was attributed to the improved dispersion of WL and KL particles in the PU system in the presence of SL (Fig. 3a). The mechanical strength of PU films was enhanced when they contained a higher concentration (5% and 10%) of KL in the presence of SL, as compared to a similar concentration with WL. There could be a possible reaction between the KL hydroxyl groups (Fig. S2c) and the isocyanate groups, resulting in the formation of urethane bonds and contributing to improved mechanical strength.[58] This phenomenon is not applicable to WL, as siloxane groups occupy the hydroxyl groups (Fig. S2c). However, when the concentration of KL increased beyond 10%, the tensile strength decreased, even in the presence of SL. Consequently, producing a PU film with a concentration exceeding 10% in KL material was deemed unattainable (Fig. S8).

Nevertheless, it was possible to produce a film with higher concentrations of WL (25% and 50%) despite the subsequent reduction in mechanical properties.

According to the data presented in Fig. S7d, it can be observed that the elongation at the break of the PS-containing film was comparatively lower than that of PKL10S and PWL10S. Additionally, the elongation at the break of KL and WL-containing films with SL films exhibited a steady drop as the KL or WL content concentration increased. The increase in KL or WL in the PU matrix would increase the PU composite matrix's hard segment, reducing the PU film's affinity to deform under stress and making it more brittle with a decrease in elongation at break.[58,59]

The thermal stability of PS, PKL10S, PWL10S, and PWL50S was investigated, and their TGA and DTG curves are shown in Fig. 4e and f, respectively. Except for PWL50S, which exhibited a 60 °C rise in the T_o compared to PWL50 (Fig. 2i and j), the remaining samples did not demonstrate an increase in the T_o. This result indicates that the introduction of SL had no impact on the thermal resistance of PKL10 or PWL10 but had a notable effect on PWL50, where the concentration of WL was higher (50%). This enhancement was directly related to the dispersion of WL in the PU system due to the presence of SL (Fig. 2a).

Notably, in the absence of SL in the formulation, the T_o was significantly lower (Fig. 2a). The SL films demonstrated elevated temperatures at $T_{50\%}$ compared to the formulation without SL. The experimental findings demonstrated temperature enhancements of 24, 10, 44, and 54 °C for PS, PKL10S, PWL10S, and PWL50S, respectively. This indicates that more energy was required to break the interaction between KL or WL and PU chemical chains in the presence of SL. The inclusion of SL also improved the DTG_{max} for all the films. Nevertheless, the DTG_{max} of PKL10S exhibited a higher increase than PWL10S and PWL50S. In this case, SL increased the composite film's KL and WL dispersion, as well as the presence of stiff phenylpropane aromatic rings. This improvement in thermal stability was achieved by increasing char formation. Typically, the dense organization of lignin within the PU matrix can significantly enhance the heat resistance of the films.[60] It is worth mentioning that WL particles were also beneficial for increasing the residual weight of the PU films, as expected.

After SL was incorporated into the PU films, the LOI value was investigated for samples of PS, PKL10S, PWL10S, and PWL50S. The PS film demonstrated a 2.8% increase in LOI compared to pure PU. The LOI value for PWL50S showed a 2.2% improvement compared to the sample without SL. This improvement in the LOI value is attributed to the well-dispersed SL in the PU matrix structure (Fig. 3a). This finding is also supported by the improved thermal stability observed in the TGA analysis (Fig. 4e and f). The LOI value of 26% for PU-based film closely resembles that of a flame-retardant PU film produced by incorporating cyclotriphosphazene into PU materials.[61] However, the current study is more favorable due to the utilization of a biobased flame retardant, specifically lignin.

The UL-94 test was conducted to evaluate the flame retardancy of the samples made from PU, PS, and PWL50S, and the results are illustrated in Fig. 4h–j. When exposed to propane gas, PU underwent a consistent and sustained ignition, with a flame that burned the samples entirely within 7 seconds. Such results indicate the high flame affinity of PU films. PS samples took 12 s for the flame to propagate and reach the end of the film, but unlike PU, the PS samples left a residue of the film hanging after the flame was extinguished in 12 s. This indicates that the introduction of SL into the PU matrix, even at a 0.12 wt% concentration, improved the stability of the film when burned, as observed in the TGA and LOI analyses (Fig. 4e–g). The PWL50S films, on the other hand, took 30 seconds for the flame to reach the end of the film from the ignited tip on the second ignition. After the flame reached the top, the film still hung without losing its structural integrity. The combustion performance of PWL50S films is classified as 5VB in the UL-94 materials flame retardant categories, which stipulates that samples must cease burning within 60 seconds on a vertical specimen without dripping and may form a hole to be categorized as flame retardant.[62] This stability of PWL50S for flame is attributed to the highest concentration (50%) of WL, which has a high thermal stability (Table S1). It is worth noting that the mechanical characteristics of the material as a free-standing film may be constrained owing to reduced elasticity (Fig. 4d), perhaps arising from the elevated concentration of the hard segment (*i.e.*, lignin). This limitation was addressed using plasticizers, as seen in Fig. 5. Among several plasticizers (glycerol, tannic acid, and epoxidized oil) at a concentration of 1% in the formulation, epoxidized oil demonstrates superior performance, yielding a tensile strength of 7 ± 0.3 MPa and a percentage elongation of 106.95 ± 12.05%. This performance is promising for film applications that need more elasticity. The results indicate that epoxidized oil exhibits superior plasticization to glycerol and tannic acid in PU at the same concentration. This interaction likely arises from the reactive epoxy groups of epoxidized oil forming covalent bonds with the isocyanate groups of PU, thereby enhancing compatibility and minimizing phase separation, while its long aliphatic chains contribute to flexible molecular spacing.[63] Conversely, the diminutive size and elevated hydroxyl functionality of glycerol may facilitate excessive crosslinking.[64] Such results would lead to the stiffening of the films, while the voluminous polyphenolic

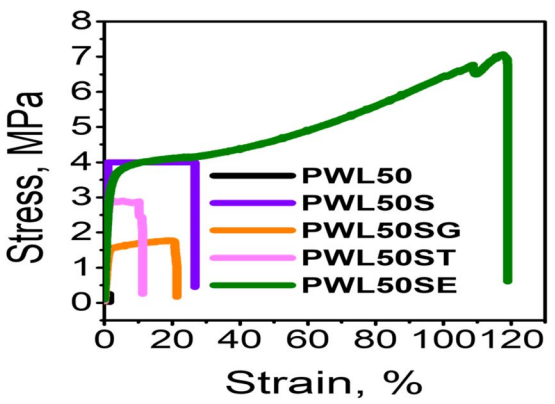

Fig. 5 Effect of plasticizers in PWL50S to improve the mechanical properties.

structure of tannic acid could impede chain mobility due to robust hydrogen bonding, hence diminishing plasticization efficiency.[65] Interestingly, the formulation without a plasticizer (PWL50S) is still adequate for coating applications, as higher elasticity is not essential.

2.6. Coating performance of lignin-silsesquioxane copolymer containing PU films

The formulation PWL50S was coated on wood, metal, and paper, and the contact angle was measured and reported using different liquids (Fig. 6a). The coated surfaces exhibited a water contact angle greater than 150°, demonstrating the superhydrophobic characteristics of the formulation. The contact angle decreased when a droplet of 0.1 M NaOH was applied. However, the variation in contact angle was less pronounced with a droplet of 0.1 M HCl. The reduced contact angle with NaOH droplets could be a result of the ionization of lignin's acidic groups (phenolic hydroxyl groups for SL) and the reduced ether bonds resulting from the presence of higher alkyl chains on WL (Fig. S2).[66] A superhydrophobic coating's durability depends on its abrasion resistance.[67] To enhance practical applicability, the superhydrophobic (PWL50S) coated wood, metal, and paper underwent sandpaper abrasion testing, and the water contact angle after abrasion was reported in Fig. 6b. The coating withstood up to 160 cm of abrasion before the contact angle dropped for wood and metal, while the coated paper failed after 60 cm.

The potential cause for the stability of superhydrophobicity on wood and metal is attributed to the strong adhesion of the coating formulation, resulting from the sticky nature of PU on metal and wood, whereas the paper itself lacks mechanical strength.[68] Following the 160 cm abrasion, the contact angle decreased for wood, but the superhydrophobicity remained unchanged on the metal surface until 320 cm. This phenomenon can be explained by the separation of the coating from the underlying wood substrate, which then exposed the wood

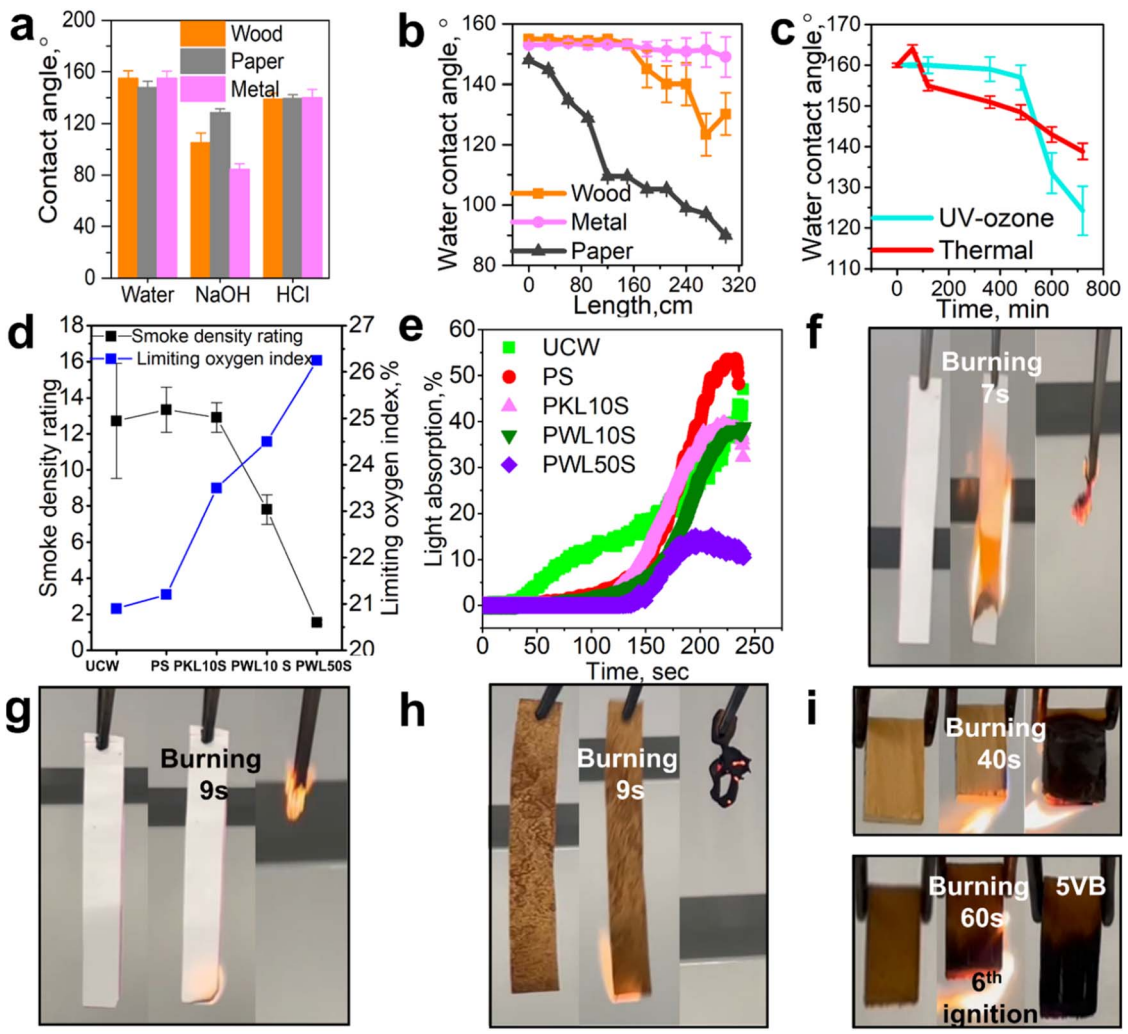

Fig. 6 Liquid contact angle (a) water contact angle after abrasion (b) of PWL50 coated wood, metal, and paper, stability of water contact angle on PWL50S coated wood after thermal exposure at a 200 °C oven and UV-ozone exposure (c), limiting oxygen index and smoke density rating (d) and light absorption (e) of PS, PKL10S, PWL10S, and PWL50S, UL-94 test on uncoated (f), PU coated (g), and PWL50S coated filter paper (h), and uncoated, PU coated and PWL50S coated wood (i).

surface directly to water droplets. The presence of the coating on the metal surface may be attributed to the metal's superior mechanical strength compared to wood.

The coated wood exhibited stability in its superhydrophobic qualities, even after being subjected to heat deterioration at 200 °C and exposed to UV-ozone for up to 200 min (Fig. 6c). The WCA remained higher than 130° even after 600 min of UV-ozone and thermal exposure. The stability of the superhydrophobic coating on wood, when exposed to thermal and UV radiation, is attributed to the thermal stability of WL and its ability to absorb 100% of UV rays. This conclusion is based on the findings of TGA and UV-vis transmittance analysis. These properties enable the coating to retain its superhydrophobicity and shield the coated wood from thermal and UV degradation. Additionally, the fire-resistant properties of the formulations were evaluated by measuring the LOI and smoke density. The LOI, SDR, and light absorption curves for uncoated wood, PS, PKL10S, PWL10S, and PWL50S coated wood are shown in Fig. 6d and e.

Concentrated smoke reduced perceptibility, limiting egress and injuring those trying to evacuate.[69] The smoke generation level of materials is a significant focal point in assessing fire safety risks.[70] Fig. 6e shows how light absorption in uncoated wood increased when lit and stabilized as it burned. Peak light absorption was 50%, and smoke density was 18 at 250 s (Fig. 6d). Wood coated with PU had a peak light absorption of 55% and a smoke density of 15. Due to their high flammability, PU coatings were unsuitable for use on naturally flammable wood. Utilizing PWL10S or PKL10S did not increase smoke production in the coated wood. Smoke output decreased when WL was increased to 50. This was supported by 29% light absorption and a smoke density of 4.

The results indicate that WL greatly reduced wood combustion. WL50 may create a cross-linked ceramic phase during burning, thereby reducing the combustion rate. This phase prevents the fire from spreading and preserves the wood's structure. UL-94 vertical burning tests were performed on uncoated paper and wood samples with PU and PWL50S. The results of these tests are presented in Fig. 6i. Uncoated and PU-coated paper burned rapidly, with the flame consuming the paper in approximately 9 and 11 seconds, respectively. In contrast, the PWL50S-coated paper self-extinguished upon initial ignition, and it took 20 seconds for the flame to spread and reach the end of the paper.

Additionally, there was a noticeable amount of paper residue left after the experiment. Uncoated and PU-coated wood immediately caught fire and burned entirely at 51 and 40 seconds, respectively, after ignition (Fig. 6f–i). However, due to its self-quenching properties, the PWL50S-coated wood required a sixth ignition. Even after the 6th ignition and 75 seconds of burning, the flame did not consume half of the coated wood, which qualifies it for the 5VB category under the UL-94 test. The self-quenching property exhibited by both paper and wood may be attributed solely to the flame retardant and thermal stability of the PWL50S coating formulation, as demonstrated in the film (Fig. 4j), as well as the higher thermal stability of WL and the charring characteristics of lignin (Table S1).

2.7. Recyclability of lignin-silsesquioxane copolymer containing PU films

The manufacture of PU is criticized for generating non-biodegradable waste in landfills, primarily due to the permanent, interconnected structure of PU crosslinks. Nevertheless, the hydroxyl and carbamate groups from polymer chains can engage in transcarbamoylation processes, creating dynamic covalent networks. These networks can undergo reversible formation and cleavage, providing PU with solvent reprocessing ability (Fig. 7).[71]

The recyclability of the PU films was examined by cutting the cured samples into smaller pieces and dissolving them in DMF. The dissolved material was cast and cured, as seen in Fig. S9. The tensile stress–strain curve of the reprocessed samples is assessed (Fig. S7f). Table 2 presents the tensile strength, elongation at break, modulus, and water contact angle of the original and recycled films. As we stated previously, commercial PU is not easily recyclable, and water-based PU has generally weaker strength than solvent-based ones. Interestingly, the system we developed in this work generated PU derivatives in aqueous systems that were recyclable in DMF. For the lignin included samples, they were recyclable due to the advantageous presence of a significant amount of hydroxyl groups in lignin. The hydroxyl groups rapidly engage in transcarbamoylation interactions with carbamate groups in a suitable solvent, resulting in the swift restoration of covalent cross-linking networks. Also, we were able to generate lignin incorporated PU formulation with similar strength, but improved hydrophobicity and flame retardancy.

Furthermore, the findings demonstrated that recycled films enhanced tensile strength and modulus. The enhanced mechanical characteristics of the films after reprocessing, as opposed to the first synthesized samples, may be attributed solely to the improved compatibility of the dispersion medium, DMF, in contrast to the original water used during the initial synthesis. The structural analysis of the films before and after reprocessing *via* FTIR (Fig. S10a and b) revealed that the characteristic peaks of the carbamate (C=O) vibrational band (1700–1730 cm^{-1}), the crosslink stretching vibrations (C–O–C),

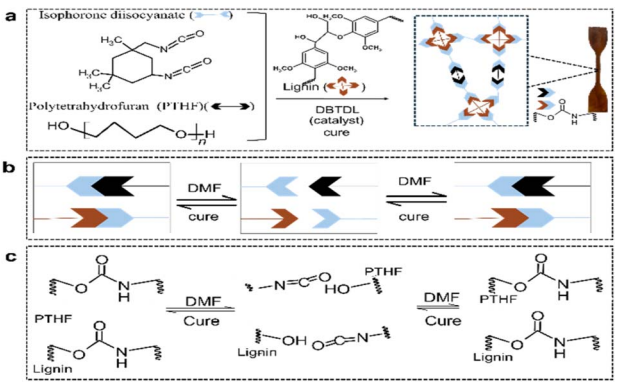

Fig. 7 Schematics of lignin-PU films illustrating the synthesis of films (a) and the dynamic bond exchange of carbamate bonds in PU networks (b and c).

Table 2 Elongation, tensile strength, and modulus of PU films for both virgin and recycled materials[a]

	Elongation, %		Tensile strength, MPa		Modulus, MPa		Contact angle, °	
Sample	Virgin	Recycled	Virgin	Recycled	Virgin	Recycled	Virgin	Recycled
PU	82.6 ± 3.5	300 ± 50	2.5 ± 0.5	39 ± 1.2	74.6 ± 4.9	22.7 ± 3.1	90 ± 3	90 ± 0.3
PS	50 ± 3.6	59.1 ± 0.6	4.5 ± 0.1	9.64 ± 0.4	209 ± 149	796.9 ± 151	90 ± 2	90 ± 0.5
PKL10S	85 ± 3.9	56.1 ± 10	14.9 ± 3	47.35 ± 5	584.5 ± 123	2006.3 ± 22	30 ± 2	29 ± 5
PWL10S	74.3 ± 8.4	9.3 ± 0.5	3.9 ± 0.7	39.8 ± 2	350 ± 166	592.6 ± 157	140 ± 3	142 ± 3
PWL50S	20.4 ± 9.5	10.7 ± 4.5	2.4 ± 0.2	10.2 ± 0.1	92.7 ± 41	447.1 ± 2.6	158 ± 2	160 ± 3

[a] The term "virgin" refers to the specimens in their as-prepared state.

and N–H stretching bands were intact in the reprocessed films. Furthermore, the DSC graph of PU, PS, and PWL50S before and after reprocessing is depicted in Fig. S11a and b. The samples' melt temperatures (T_m) didn't change significantly, while a significant shift in glass transition temperatures (T_g) was observed for all samples.

The T_g of the initially manufactured PU varied between −34.9 °C and 0.61 °C in the reprocessed samples. Similarly, the T_g of PS changed from −41.6 °C to 0.53 °C, and the T_g of PWL50S changed from −35.1 °C to −15.5 °C. The rise in T_g signifies an augmentation in crystallinity and crosslinking after reprocessing the films, potentially arising from a more organized structure in the PU polymer that would restrict molecular movement.[72]

This alteration is noteworthy in PU and PS; however, the modification in PWL50S was comparatively less pronounced. Including DMF in the recycling process may impede the movement of polymer chains due to intensified solvent–polymer interactions, resulting in an elevated T_g. In contrast, the original synthesis formulation used water, which may not facilitate strong interactions, leading to a decreased T_g. The improved higher crystallinity, as indicated by higher T_g after reprocessing, is consistent with the improved mechanical properties of the films (Table 2 and Fig. S7f).[73]

The significantly improved Young's modulus and T_g of the reprocessed film, compared to the original water-based film, are mostly attributed to dissolution in DMF, promoting molecular-level dispersion of lignin in the polyurethane matrix. In opposition to potential aggregation in water, the dissolution in DMF promoted uniform mixing that enhanced interfacial contact area and strengthened hydrogen bonding interactions between the hydroxyl groups of lignin and the polar groups of polyurethane (*e.g.*, urethane carbonyls) (Fig. S10b). The enhanced adhesion facilitated effective stress transfer, augmenting mechanical strength, while the uniformly dispersed lignin molecules function as nanoscale physical crosslinks, significantly restricting polyurethane chain mobility and leading to the observed increase in T_g.[74] Moreover, DMF's processing likely eradicated any residual water present in the initial film, thus nullifying its plasticizing effect, resulting in a greater modulus.[75]

The solvent-reprocessing affinity of PU presents a considerable recycling benefit compared to unprocessable, permanently crosslinked PU, as its dynamic or selectively cleavable bonds permit complete dissolution in designated solvents, facilitating the retrieval of pristine polymer chains for direct reutilization in high-quality PU products.[76] Conversely, unprocessable PU, *i.e.*, the characteristic of conventional thermosets, contains irreversible crosslinks that inhibit dissolution or melt-processing, significantly constraining recycling alternatives of the matrix.[77] The selection of DMF as a reprocessing solvent of the lignin incorporated PU was made to analyze fundamentally if the sample can be recycled. However, DMF is not environmentally benign. Thus, it is recommended to contemplate the adoption of green solvents when recycling/reprocessing of lignin-incorporated PU is studied at a commercial scale in the future.

2.8. Implications

The primary focus of research on PU polymers revolves around the following problems: (1) increasing the use of bio-based polymers in PU synthesis, (2) enhancing the thermal stability and recyclability of PU, and (3) increasing the hydrophobicity of PU materials.[9] One of the significant issues of including biopolymers in PU is that the performance of the final material, such as hydrophobicity, drops significantly.[69] Similar to the current study, the water contact angle values of PU films were improved in another study. However, the formulation included non-biobased ingredients, such as silicide and fluoride.[78–80] In the past, lignin was used as a filler in the production of PU film in limited quantities due to the negative impact of lignin on PU qualities (Table 3). The current study employed 50.12% of modified lignin (WL and SL) in PU formulation with superhydrophobicity and improved thermal stability and flame retardancy. Based on the proportion of pristine lignin in WL and SL (as shown in the SI), the overall proportion of pristine lignin in the PU formulation was 25.06%, which is significantly more than the previously reported results (Table 3).

A further noteworthy finding of this study is that KL at a concentration of 10 wt% was integrated into a PU film in the presence of a lignin-based dispersant, SL. This suggests that the affinity of lignin and its incorporation into a PU formulation would be improved not only by its functionalization but also by employing its derivative as a dispersant.

In short, compared with pure waterborne PU film, the lignin incorporated PU film exhibited improved hydrophobic and flame retarding performance when the same fabrication procedure is followed (Table 2). Therefore, if our suggested

Table 3 Comparing lignin concentration, tensile strength, water contact angle, and limiting oxygen index value from this work and existing work[a]

Composition	Method of lignin modification	Maximum lignin concentration, %	Tensile strength, MPa	WCA, °	LOI, %	Reference
Industrial alkali lignin, ZnO, PU	Quaternization (QAL) QAL/ZnO composite	1.2	25	✗	✗	20
Kraft lignin, 29.45 μm particle size, and WPU	Silanization with 3-aminopropyltriethoxy silane 99%	2	7	✗	✗	21
Lignin, PU, DMAc	Unmodified	3	57	110.3	✗	81
Kraft lignin, TiO_2, water-based PU	Sulfonation	2.8	9.9	85.9	✗	82
Lignin, isocyanate	Lignin urethane modification	30	13.3	✗	✗	69
Lignin, amine-modified silica, and isocyanate	Lignin liquefaction	3	9.2	73.2	✗	83
Lignin, WPU	Lignin nanoparticles	5	58	114	✗	17
WPU	Water-based PU	0	8	✗	✗	21
Kraft lignin, WPU	Silanization, sulfoethylation	50.12	7.3	150	26	This work

[a] "✗" means not reported.

formula were adapted into the PU manufacturing process, the properties of the fabricated PU film would likely be improved. In future studies, efforts should be made to adapt the suggested formulation of lignin-incorporated PU film into the commercial PU manufacturing process as the next step to fabricate the generated sustainable PU film and to understand the benefits of the developed process at commercial scales.

3. Experimental section

3.1. Materials

Kraft lignin (KL) was obtained from FPInnovations and produced *via* LignoForce technology. Aminopropyl/methyl silsesquioxane (WAPMSS) was purchased from Gelest Inc. USA. Sodium 2-bromoethanesulfonate, sodium hydroxide (NaOH), deuterated sodium hydroxide (NaOD), deuterium oxide (D_2O-d_2), deuterated dimethyl sulfoxide (DMSO-d_6), hydrochloric acid (HCl) 37%, sodium hydroxide (NaOH), 2-chloro-4,4,5,5-tetramethyl-1,3,2-dioxaphospholane (TMDP), chloroform ($CDCl_3$), ethanol (95%), pyridine, cyclohexanol (99%), chromium(III) acetylacetonate (97%), dimethylformamide (DMF), poly tetrahydrofuran (PTMG, Mw of 2000 g mol^{-1} with hydroxyl value of 204 mmol g^{-1}), isophorone diisocyanate (IPDI), monopotassium phosphate (KH_2PO_4), disodium phosphate (Na_2HPO_4), ammonium chloride (NH_4Cl), sodium chloride (NaCl), potassium hydroxide (KOH), calcium chloride ($CaCl_2$) glycerol, tannic acid, and epoxidized oil were all purchased from Millipore Sigma, Oakville, Canada. Also, nylon membrane syringe filters with 0.45 μm pore-opening filter papers were purchased from Fisher Scientific, Ottawa, Canada. A dialysis membrane (1000 g mol^{-1} cut-off) was obtained from Spectrum Labs. Stain-grade pine wood and metal sheets were purchased from Home Depot, Canada.

3.2. Preparation of KL-WAPMSS (WL), sulfoethylated lignin (SL), and PU emulsion

The polymerization of KL and WL was conducted in an aqueous environment following the polycondensation reaction.[84] The sulfoethylation of KL was also carried out following the literature.[85] The synthesis of PU was conducted using the procedure outlined in another work.[17] Information regarding the reactions is available in the SI.

3.3. Formulation development

A specific quantity of WL powder and PU emulsion was introduced to a dried vial. Then, the blend was vortexed at high speed for 5 minutes, followed by magnetic stirring at 500 rpm for 5 hours at room temperature. The mixture was named PWL*x*, where *x* represents the weight percentage of WL (3%, 5%, 10%, 25%, and 50%) in the formulation. Control samples were prepared using KL and pure PU emulsion following the same procedure.

In a different set of experiments, SL was utilized as a dispersant. It was added directly to the prepared blend of PWL50, vortexed at high speed for 5 minutes, and followed by homogenization using an ultrasonic machine (Omni-Ruptor 4000, Omni International Inc.) at room temperature, 240 W power, and 30 seconds with 3-second intervals. A varying amount of SL (0.12 wt%, 0.18 wt%, 0.25 wt%, and 0.5 wt% based on the total weight of the formulation) was added to the system to study the effect of dispersant concentrations on the formulation. The optimal concentration of SL in the formulation was determined by conducting a suspension stability test using a Turbiscan Lab Expert, following the Turbiscan Stability Index (TSI) and water contact angle analysis. This concentration was subsequently used in all samples. The samples were labeled as PWL/KL*x*S, where *x* denotes the weight percentage of WL (3%, 5%, 10%, 25%, and 50%), S represents 0.12 wt% of SL, and similarly, PS symbolizes the equivalent quantity of SL in PU.

The effect of plasticizer in PWL50S formulation was evaluated using 1 wt% glycerol, tannic acid, or epoxidized oil, followed by homogenization using an ultrasonic machine with a 240 W power setting and 30 seconds with 3-second intervals. The samples were labeled as PWL50SE for epoxidized oil, PWL50ST for tannic acid, and PWL50SG for glycerol.

3.4. Film casting and coating

For film fabrication, the formulation mixture was poured into a silicon mold, cured into a film at 55 °C, and then dried at 120 °C for 2 h. On the other hand, a formulated solution was applied to wooden, metal, and filter paper substrates. Before applying, the wood and metal surfaces were thoroughly cleaned with deionized water and then dried in an oven at 60 °C for 2 h. The wood, metal, and filter paper samples were immersed in the prepared coating solutions for 5 min and then subjected to a curing process at 120 °C for 2 h. The control samples consisted of uncoated samples and PU.

3.5. Recycling

The recyclability of the films was evaluated by inserting the cured films into a vial containing a DMF solvent and subjecting them to magnetic stirring at 250 rpm for 24 h. Subsequently, the films were produced according to the procedures outlined in Section 3.6.

3.6. Characterization

3.6.1. Structural analysis of KL, WL, and SL. KL, WL, and SL were investigated for their chemical structures using proton nuclear magnetic resonance (^{1}H-NMR), heteronuclear single quantum coherence NMR (HSQC), and ^{31}P-NMR,[45] using TopSpin 4.02 software (Bruker AVANCE Neo NMR-500 MHz apparatus USA). The details of the analysis, conditions, and sample preparation are stated in the SI. The chemical compositions of lignin polymers (KL, WL, and SL) PU composite films were examined using an XPS analyzer (Kratos AXIS Supra, Shimadzu Group Company, Japan) with a dual anode AL/Ag monochromatic X-ray source (1486.7 eV). Samples were analyzed by XPS using a double-sided carbon tape after being oven-dried at 60 °C. Steps, dwell, and sweep times were 230, 260, and 60 s. ESCApeTM (1.4.0.1149) (Kratos Analytical, Japan) was utilized to obtain spectra and quantify chemical bonds.[86]

3.6.2. Formulation stability analysis. The stability of the formulation was analyzed by taking 25 mL of the coating formulation in cylindrical glass vials. The vials were then scanned by a suspension stability analyzer called a Turbiscan lab expert (Formulation, France) every 30 s for a period of 12 h at 30 °C.[87]

3.6.3. Mechanical and thermal properties analysis of films. The mechanical properties of the PU composite films were examined using universal testing equipment with a 200 N load cell (Shimadzu Instron-6800 series, Japan).[80] The thermal stability and degradation temperatures of KL, WL, SL, PU, and PU composite films were investigated using a thermogravimetric analysis (TGA) instrument (TGAi1000, Instrument Specialists Inc., WI, USA). The glass transition (T_g) and melt temperature (T_m) for as-synthesized and recycled PU, PS, and PWL50S films were investigated *via* a differential scanning calorimeter (DSC) (DSC Q2000, TA Instruments, DE, USA). Information regarding the above characterizations is available in the SI.

3.6.4. Liquid contact angle, water absorption, and UV transmittance analysis. The static liquid contact angle investigation (water, 0.1 M NaOH, and 0.1 M HCl) utilized an optical tensiometer (Theta Lite, Bolin Scientific, Finland) equipped with a digital camera and a manual tilting stage. The films' water absorption characteristics were assessed by a force tensiometer (Attention Sigma 700/701, Biolin Scientific, Finland) with a metal probe. The study was conducted by immersing a cylindrical metal tube with an open bottom base containing 0.01 mg of the films into a liquid. The amount of liquid absorbed by the films was determined using the Washburn technique, eqn (1).

$$W^2 = \frac{C\rho\gamma l\cos\theta t}{2\eta} \quad (1)$$

where W is the weight of absorbed water (g), C is a geometric constant (0.04), ρ is the liquid density (0.998 g mL^{-1}), γ is surface tension (72.8 mN m^{-1}), l is the length of the powder glass probe (5.5 mm), η is the viscosity of the liquid (0.01 g cm s^{-1}), and t is measurements time (300 s). The UV transmittance of the films was evaluated using a UV-vis spectrophotometer (UV-2600i, SHIMADZU, Japan). The transmittance in the wavelength range of 200–800 nm was analysed. Information regarding the above characterization is available in the SI.

3.6.5. Durability of samples for abrasion, thermal, and UV-ozone. A wood, paper, and metal sample, which had been previously coated with PWL50S, was sandpapered with 1500 mesh sandpaper. A 20 g weight was then placed on top of the samples, and they were pushed down a straight line. Water contact angle analysis was conducted after each 30 cm length of abrasion. To analyze the superhydrophobicity of coated wood after thermal exposure, the previously coated wood samples were subjected to a temperature of 200 °C in an oven. The water contact angle of the samples was then measured at different time intervals. Similarly, the wood samples coated with a protective layer were also subjected to UV-ozone exposure for 800 minutes, and the water contact angle was assessed every 100-minute duration. Subsequently, the water contact angle of the samples was evaluated.

3.6.6. Ignition performance of films and coated samples. An ASTM D 2843-99 method was employed to determine the smoke emission parameters of coated wood by analyzing the smoke production profile using a smoke density test apparatus (AIC-2843, Advanced Instrument Co., Ltd, China). The limiting oxygen index (LOI) analyzer (NETZSCH TAURUS apparatus, Germany) was used to determine the lowest oxygen concentration required to ignite film samples, as per ASTM D2863.[88] The vertical burning test (UL94) as per ASTM D3801 was employed to evaluate the flame-retardant properties of the films, coated paper, and coated wood. Information regarding the above characterization is available in the SI.

4. Conclusion

A novel water-based, superhydrophobic polyurethane (PU) film was prepared using lignin and a PU water emulsion. The produced film had improved flame retardancy and recyclability

compared with pure PU film. In two different pathways, KL was utilized to generate a superhydrophobic and flame-retardant material, as well as a dispersant for single-use applications in the PU formulation. The polymerization of KL and aminopropyl/methyl silsesquioxane (WAPMSS), as well as the existence of a C–O–Si linkage, was confirmed by NMR, XPS, and FTIR techniques. Introducing WL (50 wt%) to an aqueous PU emulsion improved WCA and SA values by 60° and 4°, respectively. In the PU matrix, WL particles formed nano- and micro-air pockets (as observed *via* SEM), promoting surface superhydrophobicity. However, due to poor dispersion and aggregation of WL particles, the PWL50 film had lower mechanical strength than pure PU. Incorporating SL (0.12 wt%) as a dispersant in the PU formula increased both tensile strength and elongation while maintaining the superhydrophobicity of PWL50S with a water contact angle of 158 ± 2° and a sliding angle of less than 10°. SL also enhanced the thermal stability of PWL50S by a 31° rise in the $T_{50\%}$ compared to PWL50. The inclusion of 1 wt% epoxidized oil as a plasticizer in the formulation of the PWL50S film enhanced its mechanical properties, demonstrating that the film can be utilized as a free-standing material. In addition, the LOI value increased from 18.5 to 21% when 0.12 wt% SL was incorporated into PU, and from 24.5 to 25.5 when SL was incorporated into PWL50. PWL50S coated wood, metal, and filter paper exhibited superhydrophobic characteristics for water, NaOH (0.1 M), and HCL (0.1 M) droplets. Moreover, wood coated with PWL50S had a higher LOI and a lower SDR than PU and PKL10. In addition, the films exhibit exceptional recyclability when reprocessed and cured with a solvent, maintaining their mechanical strength and water contact values. The superhydrophobic characteristics of the coated wood remained intact after being subjected to sandpaper abrasion (160 cm), UV-ozone exposure (600 min), and thermal exposure (200 °C for 500 min). The findings of this study demonstrate that lignin can be integrated into PU films at a significant proportion (>25 wt%). Incorporating lignin imparts unique superhydrophobicity, thermal stability, and improved flame retardancy to the films and wood coatings. This, in turn, reduces the environmental impact of PU-based materials and opens possibilities for using this lignin-incorporated PU in other applications beyond coating, pending future larger-scale studies to debottleneck the potential scale-up challenges and determine the operation and capital investments of the new lignin-incorporated PU technology.

Author contributions

Banchamlak Bemerw Kassaun: experimental, conceptualization, manuscript-first draft. Yu Liu: manuscript revision, methodology. Fangong Kong: manuscript-revision, methodology. Pedram Fatehi: revision, supervision, manuscript revision. All authors reviewed and approved the submission of this manuscript.

Conflicts of interest

The authors declare no financial and non-financial conflicts of interest.

Data availability

No software or codes were used in this article, and extra data can be obtained upon request from the corresponding author.

The data supporting this article have been included as part of the supplementary information (SI). Supplementary information: methodology, chemical characterization and material performance of the generated samples. It contains 1 table and 11 figures. See DOI: https://doi.org/10.1039/d5ta04986e.

Acknowledgements

The Canada Research Chair, the Northern Ontario Heritage Fund Corporation, and the NSERC programs are acknowledged for their support of this work.

References

1 G. Rossignolo, G. Malucelli and A. Lorenzetti, *Green Chem.*, 2024, **26**, 1132–1152.
2 A. Das and P. Mahanwar, *Adv. Ind. Eng. Polym. Res.*, 2020, **3**, 93–101.
3 Y. Song, J. Li, G. Song, Z. Li, X. Yang, F. Ma and X. Li, *Composites, Part B*, 2024, **280**, 111457.
4 D. Yang, S. Wang, R. Zhong, W. Liu and X. Qiu, *Front. Chem. Sci. Eng.*, 2019, **13**, 59–69.
5 H. W. Engels, H. G. Pirkl, R. Albers, R. W. Albach, J. Krause, A. Hoffmann, H. Casselmann and J. Dormish, *Angew. Chem., Int. Ed.*, 2013, **52**, 9422–9441.
6 C. O. Adetunji, O. T. Olaniyan, O. A. Anani, A. Inobeme and J. T. Mathew, *Polyurethane Chemistry: Renewable Polyols and Isocyanates*, 2021, pp. 393–411.
7 R. H. Bean and T. E. Long, *Polym. Int.*, 2024, **73**, 5–8.
8 C. Li, P. Wang, D. Zhang and S. Wang, *ACS Appl. Mater. Interfaces*, 2022, **14**, 45988–46000.
9 H. Zhao, W.-C. Gao, Q. Li, M. R. Khan, G.-H. Hu, Y. Liu, W. Wu, C.-X. Huang and R. K. Y. Li, *Adv. Colloid Interface Sci.*, 2022, **303**, 102644.
10 H. Chang, E. B. Gilcher, G. W. Huber and J. A. Dumesic, *Green Chem.*, 2021, **23**, 4355–4364.
11 X. Ma, J. Chen, J. Zhu and N. Yan, *Macromol. Rapid Commun.*, 2021, **42**, 2000492.
12 L. Sun, Y. Guo, R. Ou, J. Xu, F. Gao, Q. Meng, S. Chen, C. Guo, Q. Fan and Q. Wang, *Adv. Funct. Mater.*, 2024, 2405424, DOI: 10.1002/adfm.202405424.
13 H. Chung and N. R. Washburn, *ACS Appl. Mater. Interfaces*, 2012, **4**, 2840–2846.
14 D. Zhang, J. Zeng, W. Liu, X. Qiu, Y. Qian, H. Zhang, Y. Yang, M. Liu and D. Yang, *Green Chem.*, 2021, **23**, 5972–5980.
15 Y. Chen, S. Fu and H. Zhang, *Colloids Surf., A*, 2020, **585**, 124164.

16 H. Li, Y. Liang, P. Li and C. He, *J. Bioresour. Bioprod.*, 2020, **5**, 163–179.
17 L. Wu, S. Liu, Q. Wang, Y. Wang, X. Ji, G. Yang, J. Chen, C. Li and P. Fatehi, *Ind. Crops Prod.*, 2022, **177**, 114526.
18 G. Qi, W. Yang, D. Puglia, H. Wang, P. Xu, W. Dong, T. Zheng and P. Ma, *Mater. Des.*, 2020, **196**, 109150.
19 X. Wang, R. O. Nayanathara, W. Leng, E. B. Caldona, L. Liu, R. C. Advincula, Z. Zhang and X. Zhang, *J. Agric. Food Res.*, 2022, **10**, 100452.
20 H. Wang, X. Qiu, W. Liu, F. Fu and D. Yang, *Ind. Eng. Chem. Res.*, 2017, **56**, 11133–11141.
21 Q. Y. Ng, J. H. Low, M. M. Pang and C. I. Idumah, *J. Polym. Environ.*, 2023, **31**, 688–697.
22 M. Shi, X. Wang and J. Yang, *Polym. Bull.*, 2023, **80**, 5553–5571.
23 N. L. K. Dona and R. C. Smith, *Molecules*, 2025, **30**, 2455.
24 Z. Ha, L. Lei, M. Zhou, Y. Xia, X. Chen, P. Mao, B. Fan and S. Shi, *ACS Appl. Mater. Interfaces*, 2023, **15**, 7427–7441.
25 J. Chen, H. Yang, Y. Qian, X. Ouyang, D. Yang, Y. Pang, L. Lei and X. Qiu, *ACS Sustain. Chem. Eng.*, 2023, **11**, 2613–2622.
26 H. Wang, Y.-A. Mai, W. Qiu, W. Liu, D. Yang, Z. Fang and X. Qiu, *ACS Sustain. Chem. Eng.*, 2025, **13**, 1292–1303.
27 D. Wang, Y. Shan, L. Liu, M. Diao and J. Yao, *Ind. Crops Prod.*, 2024, **208**, 117905.
28 Z. Huang, H. Wang, J. Du, X. Liu, G. Pan, X. Yin, W. Lin, X. Lin, Y. Sun, G. Yi and L. Niu, *Chem. Eng. J.*, 2023, **473**, 145423.
29 N. Ghavidel and P. Fatehi, *ChemSusChem*, 2020, **13**, 4567–4578.
30 M. Nagy, M. Kosa, H. Theliander and A. J. Ragauskas, *Green Chem.*, 2010, **12**, 31–34.
31 N. Mahmood, Z. Yuan, J. Schmidt and C. C. Xu, *Bioresour. Technol.*, 2013, **139**, 13–20.
32 D. Ibarra, L. García-Fuentevilla, G. Domínguez, R. Martín-Sampedro, M. Hernández, M. E. Arias, J. I. Santos and M. E. Eugenio, *Int. J. Mol. Sci.*, 2023, **24**, 2359.
33 X. Chen, X. Wang and D. Fang, *Fullerenes*, 2020, **28**, 1048–1058.
34 N. Ghavidel, M. K. R. Konduri and P. Fatehi, *Ind. Crops Prod.*, 2021, **172**, 113950.
35 L. An, G. Wang, H. Jia, C. Liu, W. Sui and C. Si, *Int. J. Biol. Macromol.*, 2017, **99**, 674–681.
36 H. Schmidt, H. Scholze and A. Kaiser, *J. Non-Cryst. Solids*, 1984, **63**, 1–11.
37 S. Liu, W. Cao, Y. Wang, W. Wei, L. Li, H. Jin and L. Guo, *Waste Manage.*, 2022, **153**, 240–248.
38 A. Miletić, P. Panjan, M. Čekada, L. Kovačević, P. Terek, J. Kovač, G. Dražič and B. Škorić, *Ceram. Int.*, 2021, **47**, 2022–2033.
39 M. Arefmanesh, T. V. Vuong, J. K. Mobley, M. Alinejad, E. R. Master and M. Nejad, *Ind. Eng. Chem. Res.*, 2020, **59**, 18740–18747.
40 M. Pomeroy, *Mater. Des.*, 2005, **26**, 223–231.
41 N. A. Miele, S. Volpe, E. Torrieri and S. Cavella, *J. Food Eng.*, 2022, **331**, 111123.
42 A. K. Mishra, D. Chattopadhyay, B. Sreedhar and K. Raju, *Prog. Org. Coat.*, 2006, **55**, 231–243.
43 D. Ibarra, L. García-Fuentevilla, G. Domínguez, R. Martín-Sampedro, M. Hernández, M. E. Arias, J. I. Santos and M. E. Eugenio, *Int. J. Mol. Sci.*, 2023, **24**, 2359.
44 C. Zhao, J. Huang, L. Yang, F. Yue and F. Lu, *Ind. Eng. Chem. Res.*, 2019, **58**, 5707–5714.
45 X. Meng, C. Crestini, H. Ben, N. Hao, Y. Pu, A. J. Ragauskas and D. S. Argyropoulos, *Nat. Protoc.*, 2019, **14**, 2627–2647.
46 A. Kaur, P. Chahal and T. Hogan, *IEEE Electron Device Lett.*, 2015, **37**, 142–145.
47 L. An, C. Si, J. H. Bae, H. Jeong and Y. S. Kim, *Int. J. Biol. Macromol.*, 2020, **159**, 222–230.
48 C. Jiang, H. He, X. Yao, P. Yu, L. Zhou and D. Jia, *J. Appl. Polym. Sci.*, 2018, **135**, 45759.
49 Z. Wu, H. Wang, X. Tian, M. Xue, X. Ding, X. Ye and Z. Cui, *Polymer*, 2014, **55**, 187–194.
50 Y. Zare, *Composites, Part A*, 2016, **84**, 158–164.
51 M. A. Kashfipour, N. Mehra and J. Zhu, *Adv. Compos. Hybrid Mater.*, 2018, **1**, 415–439.
52 J. O. Akindoyo, M. Beg, S. Ghazali, M. Islam, N. Jeyaratnam and A. Yuvaraj, *RSC Adv.*, 2016, **6**, 114453–114482.
53 J. C. Q. Amado, in *Thermosoftening Plastics*, IntechOpen, London, UK, 2019, vol. 2019.
54 A. Bansal, H. Yang, C. Li, K. Cho, B. C. Benicewicz, S. K. Kumar and L. S. Schadler, *Nat. Mater.*, 2005, **4**, 693–698.
55 G. Dias, M. A. Prado, C. Carone, R. Ligabue, A. Dumas, F. Martin, C. Le Roux, P. Micoud and S. Einloft, *Polym. Bull.*, 2015, **72**, 2991–3006.
56 X. Xiao, J. Jiang, Y. Wang, B. Wang, T.-Q. Yuan, Q. Shi, X. Liao, B. Shi and R.-C. Sun, *ACS Sustain. Chem. Eng.*, 2021, **9**, 9053–9061.
57 X. Li, Y. Liu and X. Ren, *Int. J. Biol. Macromol.*, 2022, **216**, 86–94.
58 B. M. Kim, J. S. Choi, S. Jang, H. Park, S. Y. Lee, J. Jung and J. Park, *Polymers*, 2023, **15**, 3987.
59 J. Huang, H. Wang, W. Liu, J. Huang, D. Yang, X. Qiu, L. Zhao, F. Hu and Y. Feng, *Int. J. Biol. Macromol.*, 2023, **225**, 1505–1516.
60 E. A. Agustiany, M. Rasyidur Ridho, M. Rahmi DN, E. W. Madyaratri, F. Falah, M. A. R. Lubis, N. N. Solihat, F. A. Syamani, P. Karungamye and A. Sohail, *Polym. Compos.*, 2022, **43**, 4848–4865.
61 Y. Fang, X. Du, S. Yang, H. Wang, X. Cheng and Z. Du, *Polym. Chem.*, 2019, **10**, 4142–4153.
62 W. Moloto, M. P. Motaung, B. Ntsendwana, T. C. Mokhena and M. J. Mochane, in *Biomaterials as Green Flame Retardants*, Springer, 2024, pp. 1–34.
63 H. Hosney, B. Nadiem, I. Ashour, I. Mustafa and A. El-Shibiny, *J. Appl. Polym. Sci.*, 2018, **135**, 46270.
64 P. Chen, H. Tian, L. Zhang and P. R. Chang, *Ind. Eng. Chem. Res.*, 2008, **47**, 9389–9395.
65 Y. Wang, S. Liu, K. Ding, Y. Zhang, X. Ding and J. Mi, *J. Mater. Chem. B*, 2021, **9**, 4746–4762.
66 E. I. Evstigneev, *Russ. J. Appl. Chem.*, 2011, **84**, 1040–1045.
67 Y. Liu, Y. Shao, Y. Wang and J. Wang, *Colloids Surf., A*, 2022, **648**, 129335.
68 S. Rabbani, E. Bakhshandeh, R. Jafari and G. Momen, *Prog. Org. Coat.*, 2022, **165**, 106715.

69 E. Pearce, *Flame-retardant Polymeric Materials*, Springer Science & Business Media, 2012.
70 L. Imhof and K. Stueben, *Polym. Eng. Sci.*, 1973, **13**, 146–152.
71 C. Bakkali-Hassani, D. Berne, V. Ladmiral and S. Caillol, *Macromolecules*, 2022, **55**, 7974–7991.
72 S. Kim, K. Li, A. Alsbaiee, J. P. Brutman and W. R. Dichtel, *Adv. Mater.*, 2023, **35**, 2305387.
73 M. I. León-Campos, J. A. Claudio-Rizo, D. A. Cabrera-Munguía, L. E. Cobos-Puc, M. Caldera-Villalobos, M. O. González-Díaz and F. J. Enríquez-Medrano, *J. Polym. Res.*, 2024, **31**, 213.
74 R. Mohammadpour and G. M. M. Sadeghi, *J. Appl. Polym. Sci.*, 2021, **138**, 49864.
75 S. Oprea, *High Perform. Polym.*, 2005, **17**, 163–173.
76 D. J. Fortman, J. P. Brutman, G. X. De Hoe, R. L. Snyder, W. R. Dichtel and M. A. Hillmyer, *ACS Sustain. Chem. Eng.*, 2018, **6**, 11145–11159.
77 H. E. Wray, S. Luzzi, P. D'Arrigo and G. Griffini, *ACS Sustain. Chem. Eng.*, 2023, **11**, 8065–8074.
78 J. Wu, X. Wu, C. Mu, C. Wang and W. Lin, *Prog. Org. Coat.*, 2024, **188**, 108174.
79 S. Dai, F. Yan, J. Ma, J. Guo, H. Hu, Y. Liu, L. Liu and Y. Ao, *Compos. Sci. Technol.*, 2024, **245**, 110328.
80 H. Zheng, M. Pan, J. Wen, J. Yuan, L. Zhu and H. Yu, *Ind. Eng. Chem. Res.*, 2019, **58**, 8050–8060.
81 W. Liu, C. Fang, S. Wang, J. Huang and X. Qiu, *Macromolecules*, 2019, **52**, 6474–6484.
82 Z. Yuan, X. Shang, J. Fang and H. Li, *Int. J. Biol. Macromol.*, 2022, **198**, 18–25.
83 B. Xue, Y. Yang, R. Tang, Y. Sun, S. Sun, X. Cao and X. Li, *BioResources*, 2019, **14**, 6100–6113.
84 B. Bemerw Kassaun and P. Fatehi, *Chem. Eng. J.*, 2024, **493**, 152582.
85 K. Bahrpaima and P. Fatehi, *ChemSusChem*, 2018, **11**, 2967–2980.
86 L.-S. Johansson, J. Campbell, K. Koljonen and P. Stenius, *Appl. Surf. Sci.*, 1999, **144**, 92–95.
87 J. Zhang, H. Cui, J. Qiu, X. Wang, Y. Zhong, C. Yao, L. Yao, Q. Zheng and C. Xiong, *Food Chem.*, 2023, **410**, 135364.
88 K. Sykam, S. S. Hussain, S. Sivanandan, R. Narayan and P. Basak, *Prog. Org. Coat.*, 2023, **179**, 107549.